# Vacancy Formation Energy in Disodium Oxide at 0K

V. P. Saleel Ahammad Saleel[1] and R. D. Eithiraj[2*]

[1,2]*Computational Material Science Lab, Department of Physics, School of Advanced Sciences, Vellore Institute of Technology, Vellore 632 014, TN, India.*

**ABSTRACT**

*A first-principles investigation for disodium oxide in a cubic lattice with $Na^+$ defect, Face center defect, $Na^+$ and $O^-$ vacancy, has been carried out by the PWscf (plane-wave self-consistent field) approach with standard local-density approximation (LDA) and generalized gradient approximation (GGA). The total energy, lattice constant, volume variations, cation defect, anion defect, vacancy defect and vacancy energy formation are calculated with relaxed supercell structure 1x1x1 of disodium oxide.The calculated total energy increases by increasing vacancy in supercell structure. $O^-$ vacancy formation energy is higher than the $Na^+$ vacancy formation energy.*

## 1.   INTRODUCTION

Imperfections in the form of defects within the crystals are commonly present. Their existence destroys the periodicity of the lattice structures in the regular ordered crystals. Among the different types of imperfections, we consider the situation in which lattice site remains vacant which are called vacancies. Oxygen vacancies energetically influence the physicochemical properties of oxide systems and are examined widely both experimentally and the hypothetically [1-4]. Metal oxides have long-lasting wide bandgap oxides with impressive technology application. Extensive experimental studies are carried out of defects in metal oxides and notably Face Centre center vacancy (also known as an O vacancy) [5-10]. Point defects, like atomic vacancies play a crucial role in tailoring the properties of metal oxides [11-15]. Atomic vacancies are impossible to avoid during sample preparation [16]. By controlling the density and distribution of vacancies, it is likely to impact their physical properties such a bandgap, conductivity, magnetism, etc. This can generate exciting applications in the fields of energy storage and physical gadgets [17]. Compounds with antifluorite crystal structure are found to show quick particle conductivity and their interesting properties useful in gas detectors, solid state batteries and energy storage [18-20]. $Na_2O$ plays necessary cutting edge role in optic, glass and ceramic application. They have force in extensive thought due to their mechanical usefulness, and moreover alternative outstanding and interesting physicochemical properties [21-26]. In the present investigation, we carry out extensive calculation for without defect , $Na^+$ defect, Face center defect, $Na^+$ and $O^-$ vacancy calculation for $Na_8O_4$ by using the Density Functional Theory (DFT) within *ab-initio* pseudopotentials method with the occupied valence orbitals represented by a plane wave expansion.

---

[*]Corresponding Author: *eithiraj.rd@vit.ac.in*

## 2. COMPUTATIONAL DETAILS

The studies were carried out under the formalism of the Density Functional Theory, using the plane wave methods and the ultrasoft atomic pseudopotentials, as it is appear in the Quantum Espresso computational code [27]. The plane wave premise was increased to an energy cut-off of 32Ry. The G vectors that permit the expansion are vectors of reciprocal lattice. At first, an infinite number of vectors are required to represent the wave functions with an infinite exactness. However, the expansion of the plane waves may be truncated to a finite number of terms, to constrain the wave functions with a lower kinetic energy than an energy cut-off $E_{cutoff}$ [28]. The local-density approximation (LDA) utilizes the Perdew-Zunger (PZ) [29] and generalized gradient approximation (GGA) utilizing the Perdew-Burke-Ernzerhof (PBE) [30] for exchange and correlation impacts. The $Na_2O$ was considered in the antifluorite crystallization phase, with a constant optimized lattice of 5.409Å, employing a k Monkhorst- Pack point mesh [31] of 4x4x4, in the first Brillouin zone. For sodium, the reference occupancy was chosen as $1s^2 2s^2 2p^6 3s^1$, while the oxygen premise orbitals are $1s^2 2s^2 2p^4$. The defect free structures of $Na_2O$ are show in Fig. 1.
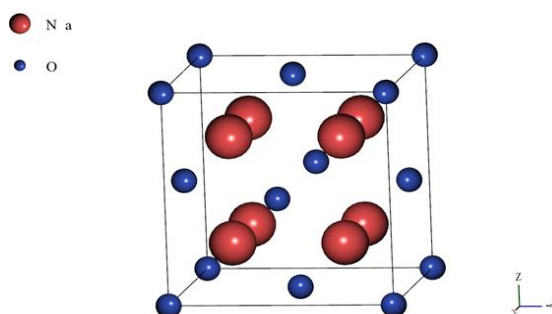


**Figure 1.** Unit Cell of $Na_2O$ antifluotie structure.

## 3. RESULTS AND DISCUSSION

### 3.1 Total Energy Calculation

We have calculated relaxed and unrelaxed total energy for imperfection free, cationic defect, F centre defect, cationic and anionic vacancy using two different functional approximations namely LDA and GGA. To create cationic defect we have moved one sodium atom site from (0.25, 0.25, 0.25) to BCC site. For F centre defect the position of oxygen atom from (0.0, 0.5, 0.5) shifted to BCC site. The sodium and oxygen vacancy are created by removing atomic site one by one. From Table 1, we observed that LDA reliably gives larger values of the total energy compared than the GGA Exc functional does and furthermore total energy increases by increasing $Na^+$ and $O^-$ vacancy in $Na_8O_4$ supercell structure.

### 3.2 Relaxed Lattice Structure

An outline of the lattice parameters relaxed structures in the ideal crystal system, Na+ defect; Facecenter imperfection and vacancy for $Na_8O_4$ supercell structure are appeared in Table 2. The calculated lattice constant for defect free structure is higher in GGA than compared LDA. The initial atomic positions and lattice are set corresponding to the cubic lattice, while during relaxed calculation, the lattice symmetries turn to tetragonal for $Na_2O_4$. We found that the lattice parameters c is higher than a (or b) in $Na_2O_4$. This can be assigned to the asymmetry of charge densies in the c plane and atom a and b - axis. The cation defect, F center defect and reaming $Na^+$ and $O^-$ vacancy concentration shows cubic lattice in relaxed structures. The higher value of lattice constant in $O^-$ vacancy indicates the significance of oxygen in the crystal framework.

**Table 1** Total energy calculation for different functional for different vacancy in disodium oxide supercell structure

| System | Total Energy (Ry.) | | | |
|---|---|---|---|---|
| | LDA | | GGA | |
| | Unrelaxed | Relaxed | Unrelaxed | Relaxed |
| $Na_8O_4$ | -896.28161940 | -896.28333369 | -897.91090681 | -897.92089483 |
| Na Defect | -896.04605947 | -896.28331942 | -897.67693619 | -897.92019866 |
| Face Centre Defect | -895.98742544 | -896.05077965 | -897.61333989 | -897.70035751 |
| $Na^+$ Vacancy | | | | |
| $Na_{(1)}$ | -800.08355245 | -800.10512247 | -801.55409977 | -801.57662958 |
| $Na_{(2)}$ | -703.91020689 | -703.91843255 | -705.2008102 | -705.22339900 |
| $Na_{(3)}$ | -607.69421612 | -607.72116550 | -608.84491872 | -608.85540753 |
| $Na_{(4)}$ | -511.44276203 | -511.53595021 | -512.42804112 | -512.49236247 |
| $Na_{(5)}$ | -415.13611937 | -415.35095952 | -415.95149475 | -416.09187446 |
| $Na_{(6)}$ | -318.84598539 | -319.59649757 | -319.43889137 | -320.04891051 |
| $Na_{(7)}$ | -222.45765297 | -223.09491590 | -222.92227329 | -223.38863079 |
| $Na_{(8)}$ | -126.08050188 | -126.88199709 | -126.36326418 | -126.92955715 |
| Anion Vacancy | | | | |
| $O_{(1)}$ | -863.98397146 | -863.99946488 | -865.57966687 | -865.62596433 |
| $O_{(2)}$ | -831.69614857 | -831.75377151 | -833.28265317 | -833.39624101 |
| $O_{(3)}$ | -799.43696413 | -799.56632495 | -801.00841145 | -801.20780455 |
| $O_{(4)}$ | -767.21327210 | -767.41598254 | -768.76989308 | -769.05504571 |

**Table 2** Lattice constant (in Å) predicted by different functional for imperfection free, $Na^+$ defect, Face centre defect, $Na^+$ and $O^-$ vacancy in disodium oxide supercell structure

| System | Relaxed Lattice Constant (in Å) | | | | | |
|---|---|---|---|---|---|---|
| | LDA | | | GGA | | |
| | a | b | c | a | b | c |
| *5.464 Å[18] | | | | | | |
| $Na_8O_4$ | 5.409 | 5.409 | 5.409 | 5.595 | 5.595 | 5.595 |
| $Na^+$ Defect | 5.409 | 5.409 | 5.409 | 5.563 | 5.563 | 5.563 |
| Face Centre Defect | 5.707 | 5.707 | 5.289 | 5.879 | 5.879 | 5.520 |
| $Na^+$ Vacancy | | | | | | |
| $Na_{(1)}$ | 5.403 | 5.403 | 5.403 | 5.593 | 5.593 | 5.593 |
| $Na_{(2)}$ | 5.392 | 5.392 | 5.343 | 5.583 | 5.583 | 5.573 |
| $Na_{(3)}$ | 5.261 | 5.261 | 5.261 | 5.490 | 5.490 | 5.490 |
| $Na_{(4)}$ | 5.077 | 5.077 | 5.077 | 5.294 | 5.294 | 5.294 |
| $Na_{(5)}$ | 5.336 | 5.336 | 5.336 | 5.515 | 5.515 | 5.515 |
| $Na_{(6)}$ | 3.985 | 3.985 | 3.615 | 4.122 | 4.122 | 3.729 |
| $Na_{(7)}$ | 3.769 | 3.769 | 3.769 | 3.968 | 3.968 | 3.968 |
| $Na_{(8)}$ | 3.068 | 3.068 | 3.068 | 3.173 | 3.173 | 3.173 |
| Anion Vacancy | | | | | | |
| $O_{(1)}$ | 5.583 | 5.583 | 5.583 | 5.764 | 5.764 | 5.764 |
| $O_{(2)}$ | 5.765 | 5.765 | 5.920 | 5.936 | 5.936 | 6.075 |
| $O_{(3)}$ | 6.097 | 6.097 | 6.097 | 6.239 | 6.239 | 6.239 |
| $O_{(4)}$ | 6.422 | 6.422 | 6.422 | 6.530 | 6.530 | 6.530 |

* Experimental Lattice Constant

## 3.3 Vacancy Relaxation Volume

From Table 3, the cation imperfection shows no volume variation in the relaxed structure when compared with defect free relaxed structure for LDA and GGA approximation.  For F centre defect both LDA and GGA approximation shows positive volume variation compared with defect free structure, which strongly indicating volume is expanding when oxygen moved to BCC lattice site.  When increasing number cation vacancy the volume continuously decreases, where us for anion vacancy volume gradually increases.  Which shows anion plays a significant role in structural arrangement.

**Table 3** Calculated equilibrium volume and volume variation of relaxed structure with different functional for imperfection free, $Na^+$ defect, Face centre defect, $Na^+$ and $O^-$ vacancy in disodium oxide supercell structure

| System | LDA | | GGA | |
|---|---|---|---|---|
| | Equilibrium Volume (in $Å^3$) | Volume Variation (in %) | Equilibrium Volume (in $Å^3$) | Volume Variation (in %) |
| *163.165 $Å^3$ [18] | | | | |
| $Na_8O_4$ | 158.252 | --- | 175.146 | --- |
| $Na^+$ Defect | 158.252 | --- | 172.158 | -1.706 |
| Face Centre Defect | 172.261 | 8.853 | 190.786 | 8.930 |
| $Na^+$ Vacancy | | | | |
| $Na_{(1)}$ | 157.726 | -0.332 | 174.958 | -0.107 |
| $Na_{(2)}$ | 155.341 | -1.839 | 165.107 | -5.731 |
| $Na_{(3)}$ | 145.622 | -7.981 | 163.057 | -6.901 |
| $Na_{(4)}$ | 130.864 | -17.306 | 148.371 | -15.286 |
| $Na_{(5)}$ | 151.931 | -3.994 | 167.739 | -4.228 |
| $Na_{(6)}$ | 57.407 | -63.724 | 63.359 | -63.825 |
| $Na_{(7)}$ | 53.540 | -66.168 | 62.476 | -64.329 |
| $Na_{(8)}$ | 28.877 | -81.752 | 31.945 | -81.760 |
| Anion Vacancy | | | | |
| $O_{(1)}$ | 174.021 | 9.964 | 191.501 | 9.338 |
| $O_{(2)}$ | 196.752 | 24.328 | 214.059 | 22.217 |
| $O_{(3)}$ | 226.646 | 43.218 | 242.853 | 38.657 |
| $O_{(4)}$ | 264.856 | 67.363 | 278.445 | 58.978 |

* Experimental Volume

## 3.4 Vacancy Formation Energy

The cation vacancy energy formation $E_c$ is calculated as;

$$E_c = E(Na_7O_4) + E(Na) - E(Na_8O_4) \tag{1}$$

Here $E(Na_7O_4)$ and $E(Na_8O_4)$ indicate the calculated total energy of the 1x1x1 supercell with cation vacancy  and  imperfection free structure individually, and E(Na) is the total energy of the free Na atom. The anion formation energy $E_a$ is  computed as;

$$E_a = E(Na_8O_3) + E(O) - E(Na_8O_4) \tag{2}$$

Here, $E(Na_8O_3)$ and $E(Na_8O_4)$ indicate the calculated total energy of the 1x1x1 supercell with anion vacancy and imperfection structure individually, and E(O) is the total energy of the free O atom in its ground state.  Table 3 shows vacancy formation energy comparison between the LDA and GGA approximation. From the  investigation of the vacancy formation energy, LDA reliably gives high values of the vacancy energy formation  values than the GGA.  The acquired values of

cation vacancy energy formation with LDA and GGA are 329 and 278 kJ/mol. The value of anion vacancy with LDA and GGA obtained are 739 and 738 kJ/mol, respectively. It was seen that anion vacancy formation energy is much higher than the cation vacancy formation energy. We likewise realize that formation energy increase with increase $Na^+$ and $O^-$ vacancy and which cause the loss of stability in the $Na_8O_4$. The investigated outcome shows mono vacancies has smallest formation energy. The vacancy energy formation changes to higher as the vacancy density increases.

**Table 4** Calculated vacancy formation energy (in kJ/mol) by different functional for $Na^+$ and $O^-$ vacancy in disodium oxide supercell structure

| System | Vacancy Formation Energy (in kJ/mol) | |
| --- | --- | --- |
| | **LDA** | **GGA** |
| **Cation Vacancy** | | |
| **$Na_{(1)}$** | 329.7803152 | 278.8077410 |
| **$Na_{(2)}$** | 670.6969481 | 569.3789269 |
| **$Na_{(3)}$** | 1025.4806820 | 879.3453859 |
| **$Na_{(4)}$** | 1364.4617713 | 1182.7998974 |
| **$Na_{(5)}$** | 1703.1418602 | 1535.4140636 |
| **$Na_{(6)}$** | 1476.6464990 | 1418.6886262 |
| **$Na_{(7)}$** | 2230.9262210 | 2112.3442801 |
| **$Na_{(8)}$** | 2606.2729975 | 2541.8667144 |
| **Anion Vacancy** | | |
| **$O_{(1)}$** | 739.5631941 | 738.4758041 |
| **$O_{(2)}$** | 1429.0115788 | 1391.3509025 |
| **$O_{(3)}$** | 2041.9964921 | 1990.0267016 |
| **$O_{(4)}$** | 2606.2729325 | 2541.8666352 |

## 4. CONCLUSIONS

We have carry out calculations for imperfection free, $Na^+$ defect, $O^-$ defect, $Na^+$ vacancy and $O^-$ vacancy calculation for disodium oxide using DFT and *ab-initio* pseudopotentials, with the occupied valence orbitals described by a plane-wave expansion. As expected, we can see that for disodium oxide the lattice parameter are slightly larger than experimental values (> 2.3%) with the GGA functional. The anion vacancy formation energy is higher than the cation vacancy formation energy. Anion plays a important role in structural arrangement. Removing $Na_{(7)}$ prompts to a more distinct relaxed geometric structure, this leads to lower vacancy formation energy when compared to $Na_{(5)}$ and $Na_{(7)}$ atomic site vacancy. From the analysis of the vacancy formation energy, LDA reliably gives higher values of the vacancy formation energy than the GGA. To begin with, there are frequently incredible trial challenges in making dependable measurements of vacancy energy formation , mostly for oxides, where energy formation are sometimes enormous. The computation results provide knowledge into the electronic response of the oxides crystal to the formation of the cation and anion vacancy.

## REFERENCES

[1]   A. I. Popov, E. A. Kotomin, & J. Maier, Nucl. Instrum. Methods Phys. Res. **268** (2010), 3084.

[2]   G. Pacchioni, Solid State Sci. **2** (2000) 161.

]3]   A. L. Shluger, A. S. Foster, J. L. Gavartin, & P. V. Sushko, in Nano and Giga Challenges in Microelectronics, edited by J. Greer, A. Korkin, and J. Labanowski (Elsevier, 2003), 151–222.

[4]   V. Ganduglia-Pirovano, A. Hofmann, & J. Sauer, Surf. Sci. Rep. **62** (2007) 219.

[5]   Y. Chen, R. T. Williams, & W. A. Sibley, Phys. Rev. **182** (1969), 960.

[6]   R. C. Whited & W. C. Walker, Phys. Rev. Lett. **22** (1969), p.1428.

[7]   L. A. Kappers, R. L. Kroes, & E. B. Hensley, Phys. Rev. B **1** (1970), 4151.

[8]   G. H. Rosenblatt, M. W. Rowe, G. P. Williams, Jr, R. T. Williams, & Y. Chen, Phys. Rev. B   **39** (1989), 10309.

[9]   A. Lushchik, T. Kärner, C. Lushchik, E. Vasil'chenko, S. Dolgov, V. Issahanyan, & P. Liblik, Phys. Status Solidi C **4** (2007), 1084.

[10]  E. Feldbach, R. Jaaniso, M. Kodu, V. P. Denks, A. Kasikov, P. Liblik, A. Maaroos, H. Mändar, & M. Kirm, J. Mater. Sci.: Mater. Electron. **20** (2009), 321.

[11]  J.-Y. Noh, H. Kim, Y.-S. Kim, Phys. Rev. B **89** (2014), 205417.

[12]  R. E. Mapasha, M. P. Molepo, R. C. Andrew, N. Chetty, J. Phys. Condens. Matter. **28** (2016) 055501.

[13]  S. Salehi, A. Saffarzadeh, Surf. Sci. **651** (2016), 215.

[14]   C. Wang, H. Han and Y. Guo, Cmp. Mat. Sci **159** (2019) 127-135.

[15]   Li Xiao-Hong, Su Xiang-Ying and Z. Rui-Zhou, RSC Adv **9** (2019) 27646-27651.

[16]  X. Sang, Y. Xie, M.-W. Lin, M. Alhabeb, K. L. Van Aken, Y. Gogotsi, P. R. C. Kent, K. Xiao, R. R. Unocic, ACS Nano **10** (2016) 9193–9200.

[17]  Guoweei Li, R. Graeme Blake & Thomas T. M. Palstra, Chem. Soc. Rev. **46** (2017), 1693.

[18]  E. Zintl, A. Harder & B. Dauth  Z. Elektrochem., **40** (1934), 588.

[19]  M. Jamal, G. Venugopal, M. Shareefudheen & M. N Chary, Mat.Lett. **39** (1999), 28.

[20]  K. I. Chao, S. H. Lee, K. H. Cho, D. W. Shin & Y. K. Sun,  J. Power Sour. **163** (2006), 223.

[21]  G. Kalpana, B. Palanivel & M. Rajagopalan, Phys. Rev. B, **52** (1995), 4.

[22]  A. Lazicki, C.S. Yoo, W.J. Evans and W.E. Pickett,  Phys. Rev. B, **73** (2006), 184120.

[23]  K. Kunc, I. Loa, A. Grzechnik & K. Syassen,  Phys. Stat. Sol. B, **242** (2005), 1857.

[24]  M. Moakafi, R. Khenata, A. Bouhemadou & H. Khachai, Eur. Phys. J. B **64** (2008), 35.

[25]  K. Bidai, M. Ameri, A. Zaoui, & I. Ameri, Ch.J. Ph. **54** (2016), 678.

[26]  R. D. Eithiraj, G. Jaiganesh, & G. Kalpana, Physica B: Con. Matter, **396** (2007), 124.

[27]  P Giannozzi, S Baroni, N Bonini, M Calandra, R Car, C Cavazzoni, D Ceresoli, G L Chiarotti, M Cococcioni, I Dabo, A D Corso, S de Gironcoli, S Fabris, G Fratesi, R Gebauer, U Gerstmann, C Gougoussis, A Kokalj, M Lazzeri, L Martin-Samos, N Marzari, en Francesco Mauri, R Mazzarello, S Paolini, A Pasquarello, L Paulatto, C Sbraccia, S Scandolo, G Sclauzero, A P Seitsonen, A Smogunov, P Umari & R M Wentzcovitch, Quantum espresso: a modular and open-source software project for quantum simulations of materials, Journal of Physics Condensed Matter **21** (2009), 395502.

[28]  J Kohanoff, Electronic Structure calculations for solids and molecules: Theory and computational methods (United Kingdom: Cambridge University Press) (2006), 382.

[29]  J. P. Perdew & A. Zunger, Phys. Rev. B **23** (1981), 5048.

[30]  J P Perdew, K Burke & M Emzerhof, Physical Review Letters. **77** (1996), 3856.

[31]  H J Monkhorst & J D Pack, Special points for brillouin-zone integrations, Physical B **13** (1976), 5188.